Published online 13 June 2017

Nucleic Acids Research, 2017, Vol. 45, No. 14 ***8609–8620***
doi: 10.1093/nar/gkx526

A data-driven structural model of hSSB1 (NABP2/OBFC2B) self-oligomerization

Christine Touma[1,†], Mark N. Adams[2,†], Nicholas W. Ashton[2,†], Michael Mizzi[1], Serene El-Kamand[1], Derek J. Richard[2], Liza Cubeddu[1,3,*] and Roland Gamsjaeger[1,3,*]

[1]School of Science and Health, Western Sydney University, Penrith, NSW 2751, Australia, [2]School of Biomedical Research, Institute of Health and Biomedical Innovation at the Translational Research Institute, Queensland University of Technology, Woolloongabba, QLD 4102, Australia and [3]School of Life and Environmental Sciences, University of Sydney, NSW 2006, Australia

Received April 20, 2017; Revised May 23, 2017; Editorial Decision June 04, 2017; Accepted June 05, 2017

ABSTRACT

The maintenance of genome stability depends on the ability of the cell to repair DNA efficiently. Single-stranded DNA binding proteins (SSBs) play an important role in DNA processing events such as replication, recombination and repair. While the role of human single-stranded DNA binding protein 1 (hSSB1/NABP2/OBFC2B) in the repair of double-stranded breaks has been well established, we have recently shown that it is also essential for the base excision repair (BER) pathway following oxidative DNA damage. However, unlike in DSB repair, the formation of stable hSSB1 oligomers under oxidizing conditions is an important prerequisite for its proper function in BER. In this study, we have used solution-state NMR in combination with biophysical and functional experiments to obtain a structural model of hSSB1 self-oligomerization. We reveal that hSSB1 forms a tetramer that is structurally similar to the SSB from *Escherichia coli* and is stabilized by two cysteines (C81 and C99) as well as a subset of charged and hydrophobic residues. Our structural and functional data also show that hSSB1 oligomerization does not preclude its function in DSB repair, where it can interact with Ints3, a component of the SOSS1 complex, further establishing the versatility that hSSB1 displays in maintaining genome integrity.

INTRODUCTION

Cell survival is contingent on the ability of cells to maintain their genomic information. Failure to protect, the genome can give rise to serious diseases such as various cancers. For this reason, eukaryotic cells have evolved to combat DNA damage with an obligation to protect genomic information. The family of single-stranded DNA binding (SSB) proteins are essential in safeguarding the integrity of DNA (1–4). SSB proteins confer genomic stability by protecting exposed single-stranded DNA (ssDNA) from degradation and aid in the detection and recruitment of vital repair proteins to the site of DNA damage, which instigates an appropriate DNA damage response (5). SSBs exist within all three domains of life and their binding to ssDNA is mediated through the oligonucleotide binding (OB) domain, which consists of five anti-parallel β-strands that are arranged into a β-barrel.

The structure of the OB domain is largely conserved across the domains of life, however the quaternary structure of SSB proteins are quite diverse. Replication protein A (RPA) is known to assemble into a heterotrimer containing six OB folds: four of which contact ssDNA, the remaining two are exclusively protein binding (6–9). The SSB from *Escherichia coli* (EcoSSB) is a homotetramer which allows ssDNA to uniquely wrap around each of the four OB domains with varying degrees of affinity (10–12). In contrast, the SSB from *Sulfolobus solfataricus* (SsoSSB) is a simple monomer containing only one OB domain that recognizes ssDNA (13–16). We have recently characterized the DNA binding properties of the OB domain from human SSB1 (hSSB1/NABP2/OBFC2B) (17). Similar to other SSB OB domains, hSSB1 utilizes a set of important and conserved aromatic residues that form stacking interactions with the ssDNA bases (17,18). The OB domain is located at the N-terminus of the protein whereas the disordered C-terminal 'tail' is known to be utilized in protein–protein interactions (3,17,19).

hSSB1 has been shown to exist in separate multi-protein complexes, such as the SOSS1 complex (consisting of hSSB1, Ints3 and C9orf80) that is essential in homologous recombination (HR)-mediated DNA repair (20–23) or the

*To whom correspondence should be addressed. Tel: +61 296859907; Email: r.gamsjaeger@westernsydney.edu.au
Correspondence may also be addressed to Liza Cubeddu. Tel: +61 246203343; Email: l.cubeddu@westernsydney.edu.au
†These authors contributed equally to this work as first authors.
Present address: School of Science and Health, Western Sydney University, Penrith, NSW 2751, Australia.

MRN complex (consisting of Mre11, Rad50 and Nbs1) that is required for the efficient resection of double-stranded breaks (DSBs) (24,25). In both of these complexes, hSSB1 exists as a monomer. However, we have recently shown that oxidation-driven self-oligomerization of hSSB1 is essential for its function in the base excision repair (BER) pathway, where its primary purpose is to aid in the removal of oxidative DNA lesions (26,27). While our recent work has also revealed that cysteine 41 plays an important role in this process, the molecular details remain elusive as the side-chain of this residue is buried deeply inside the hydrophobic core of the protein (19) and thus unable to form any intermolecular disulfide bonds.

In this study, we have utilized solution-state nuclear magnetic resonance (NMR) in combination with multi-angle laser light scattering (MALLS) to determine the structural details of hSSB1 oligomerization. Our data-driven structural model derived from our biophysical data reveals that hSSB1 is able to form a tetramer that is structurally highly similar to the tetrameric arrangement of the SSB from *E. coli.* Oligomer formation is achieved by a subset of charged and hydrophobic amino acids in addition to both surface-exposed cysteines C81 and C99. We have verified the validity of our model using mutational analysis and functional experiments. Our structural and functional data also indicate that hSSB1 self-oligomerization does not preclude binding of the protein to the SOSS1 complex via Ints3.

MATERIALS AND METHODS

Plasmids, mutagenesis, siRNA and transfection

Both GST-tagged full length hSSB1 (1–221, $hSSB1_{1–221}$) and hSSB1 OB domain construct (1–123; $hSSB1_{1–123}$) were prepared by directional cloning into pGEX-6P using the restriction enzymes BamHI and EcoRI. All $hSSB1_{1–211}$ mutants used were synthesized by GeneArt (Regensburg, Germany). The siRNA-resistant WT 3× FLAG $hSSB1_{1–211}$ mammalian expression construct has been described previously (17) and was altered by site-directed mutagenesis to form all other described 3× FLAG hSSB1 vectors using the following primers: N16D_N18D (F) 5′-TCAAGCCTGGGCTCAAGGATCTGGACCTTA TCTTCATTGTG-3′, (R) 5′-CACAATGAAGATAAGG TCCAGATCCTTGAGCCCAGGCTTGA-3′; K72A (F) 5′- GACATTATCCGGCTCACCGCCGGGTACGCT TCAGTTTTC-3′, (R) 5′-GAAAACTGAAGCGTACCC GGCGGTGAGCCGGATAATGTC-3′; D91A (F) 5′-GGCCGTGGGGGTGCCCTGCAGAAGATTG -3′, (R) 5′-CAATCTTCTGCAGGGCACCCCCACGGCC-3′; F98A (F) 5′-CTGCAGAAGATTGGAGAAGCCT GTATGGTTTATTCTGAG-3′, (R) 5′- CTCAGAAT AAACCATACAGGCTTCTCCAATCTTCTGCAG-3′; Y102A (F) 5′-GGAGAATTCTGTATGGTTGCCT CTGAGGTTCCTAACTTC-3′, (R) 5′- GAAGTTAG GAACCTCAGAGGCAACCATACAGAATTCTCC-3′; C81S (F) 5′-GGGTACGCTTCAGTTTTCAAAG GTTCTCTGACACTATATACTGGCCGTGG-3′, (R) 5′- CCACGGCCAGTATATAGTGTCAGAGAAC CTTTGAAAACTGAAGCGTACCC-3′; C99S (F) 5′-CTGCAGAAGATTGGAGAATTCTCTATGGTTTA TTCTGAGGTTCC-3′, (R) 5′- GGAACCTCAGAATA AACCATAGAGAATTCTCCAATCTTCTGCAG -3. Mammalian expression constructs were transfected using Lipofectamine 2000 (Life Technologies). Stealth siRNA targeting hSSB1 have been described previously (17) with siRNAs transfected using RNAiMax (Life Technologies).

Recombinant protein expression

$hSSB1_{1–211}$, $hSSB1_{1–211}$ mutants and $hSSB1_{1–123}$ protein expression using the *E. coli* Rosetta 2 (for BLI) or *E. coli* BL21(DE3) (for NMR) strain was induced by addition of 0.2 mM IPTG at 25°C for 16 h. Cells were lysed by sonication in 10 mM MES, pH 6.0, 50 mM NaCl, 0.5 mM PMSF, 0.1% Triton X-100. In contrast to hSSB1 purified under non-reducing conditions, proteins purified under reducing conditions additionally contained 3 mM TCEP. Following centrifugation, the supernatant was subjected to GSH affinity chromatography followed by HRV-3C protease cleavage overnight at 4°C (leaving the 5-residue stretch GPLGS at the N-terminus of the OB domain). The solution was applied to a HiTrap HP Heparin (2 × 5 ml tandem, GE) column equilibrated with NMR buffer (10 mM MES, pH 6.0, 50 mM NaCl, 3 and 0 mM TCEP for reduced and non-reduced proteins, respectively). A 500 ml linear gradient comprising 50–1000 mM NaCl was used to elute cationic proteins. Fractions corresponding to a distinct absorbance peak were analysed by SDS-PAGE, pooled, concentrated and loaded onto a Superdex-75 gel filtration column in NMR buffer or MALLS buffer (20 mM Tris, pH 7.0, 100 mM NaCl, 1 mM EDTA). ^{15}N- and $^{15}N^{13}C$-labeled hSSB1 protein was prepared using the procedure of (28) in a 5-l biofermenter and purified as described above. Protein concentrations were determined using the absorbance at 280 nm and the theoretical molar extinction coefficient for hSSB1.

Multi-angle laser light scattering (MALLS)

Size exclusion chromatography of $hSSB1_{1–211}$ coupled to multi-angle laser light scattering (MALLS) was carried out as described previously (29) in MALLS buffer. Briefly, between 250 and 500 μg of $hSSB_{1–211}$ or $hSSB_{1–211}$ mutants were applied to a Superose 12 (10/300) analytical size exclusion column (GE healthcare) at 0.5 ml/ min. MALLS was measured in tandem with size exclusion chromatography using a MiniDawn solid-state laser diode (Wyatt) measuring at three different angles (41.5°, 90° and 138.5°) at a wavelength of 690 nm. Data collection and analysis were performed with Astra Software (Zimm/Berry fitting algorithm). The molar mass was derived from the average of Mn, Mw and Mz as calculated by ASTRA. Monomeric BSA (66 kDa) was used as a reference to determine the molecular weight of the target protein.

NMR spectroscopy and data processing

NMR experiments were carried out using 0.2–1.0 mM $hSSB_{1–123}$ in NMR buffer in the presence and absence of TCEP (3 mM). Mutant $hSSB_{1–211}$ proteins (used for MALLS experiments) were prepared at concentration between 50 μM and 500 μM in MALLS buffer without TCEP.

Proton chemical shifts were referenced to 4,4-dimethyl-4-silapentanesulfonic acid (DSS) at 0 ppm. ^{13}C and ^{15}N chemical shifts were referenced indirectly to the same signal. All NMR experiments were recorded at 298 K on Bruker 600 or 800 MHz spectrometers (Bruker Avance III) equipped with 5-mm TCI cryoprobes. 1D, 2D ^{15}N HSQC and 2D ^{13}C HSQC spectra were recorded, all data were processed using Topspin (Bruker Biospin) and protein backbone resonance assignments were taken from our previous study (18). Calculation of weighted chemical shift changes was carried out as described in (30).

HADDOCK modelling

The protein structure of hSSB1 (residue 13–106 containing the OB domain) was taken from the crystal structure of the SOSS complex (PDB 4OWX) (31) and used as input for HADDOCK (32,33), together with the structure of the EcoSSB protein tetramer (PDB ID: 1SRU) (34) as a template. Molecular docking calculations were carried out in a two-stage process. In the first stage, two single hSSB1 molecules (I and II) were used to create a dimer linked by cysteine C81. Thereby, hSSB1 protein interface residues 13–20, 43–50 and 74–85 were defined as semi-flexible based on our NMR data and the EcoSSB structure resulting in a total of 40 ambiguous interaction restraints (AIRs, fixed at 2 Å). Unambiguous restraints (UIRs, fixed at 2 Å) were introduced to link the cysteines C81 together, create β-strands between molecules I and II (hydrogen bonds between 14–20, 16–18 and vice versa) as well as hydrogen bonds to keep existing intramolecular β-strands intact during the docking. Additional C2 restraints to maintain the symmetry of the dimer were used in the calculations. The energy-best structure from the first stage (out of 200 total) was subject to a further step, whereby two dimers I/II and III/IV were docked together to create a tetramer linked by cysteine C99. To achieve that, 104 AIRs (residues 13–20, 67–73 and 87–97) as well as UIRs to link C99 and maintain structural integrity of the dimer were used. In analogy to the first stage, C2 restraints were utilized to keep the overall symmetry. The 10 conformers with the lowest value of total energy of the lowest-energy cluster out of 500 total structures were analysed using standard HADDOCK protocols and PYMOL (Schrödinger, NY). The structural coordinates of the energy-lowest model structure was deposited into the Figshare data repository (DOI: 10.6084/m9.figshare.4892129) as the RCSB PDB database does not currently accept molecular models (35).

Cell culture, treatments and clonogenic survival assays

HeLa cells were maintained in Roswell Park Memorial Institute Medium supplemented with 10% foetal calf serum and grown in a humidified atmosphere containing 2% O_2 and 5% CO_2 at 37°C. Cells were transfected and seeded for clonogenic survival assays as previously described (17). Twenty four hours post-seeding, cells were treated with 0–250 μM of H_2O_2 for 30 min in serum-free medium. Colonies were stained with 4% methylene blue in methanol after 10 days and manually counted. Assays were repeated at least four times with results displayed as the average relative count ± standard error. Statistical significance was examined using a Student's *t* test with a *P* value of 0.05 considered significant.

Cell lysis and immunoblotting

Whole cell lysates were collected as previously described (26) using a buffer containing 20 mM HEPES pH 7.5, 150 mM KCl, 5% glycerol, 10 mM $MgCl_2$, 0.5 mM EDTA, 0.05% IGEPAL CA-630 supplemented with cOmplete protease inhibitor cocktail (Roche). 15–20 μg of whole cell lysate was typically separated by electrophoresis on a 4–12% Bis–Tris Plus Bolt precast gel (Life Technologies) and transferred to nitrocellulose. Blots were then blocked in 2% fish gelatin before incubation with primary antibodies. The FLAG antibody was purchased from Sigma-Aldrich (clone M2, cat # F1804), the Actin antibody from BD Biosciences (clone C4, cat # 612656), the Ints3 antibody from Bethyl (cat # A302-050) and the GAPDH antibody from Cell Signalling Technology (cat #5174). Primary antibodies were subsequently detected with IRDye 680RD or 800CW conjugated donkey secondary antibodies (Li-Cor) and visualized using the Odyssey imaging system (Li-Cor). The software ImageJ was used to measure individual signal intensities of monomer and oligomer bands, respectively, for each lane and these values were normalized to the corresponding GAPDH loading control signal. Ratios between oligomer and monomer were calculated and are depicted in the figure ($n = 3$ blots, average ± standard error).

Immunoprecipitation

Cells were resuspended in immunoprecipitation buffer (20 mM HEPES pH 7.5, 150 mM KCl, 5% glycerol, 10 mM $MgCl_2$, 0.5% Triton X-100) supplemented with 1× phosphatase inhibitor cocktail (CST, cat # 5870), 1× protease inhibitor cocktail (Sigma-Aldrich, cat # 11697498001) and universal nuclease for cell lysis (1:2000, ThermoFisher Scientific) and lysed by sonication (Vibra-Cell, 3 mm probe; Sonics and Materials) with 3 × 3 s bursts (10% output). For the immunoprecipitation of FLAG-tagged proteins, 1000 μg of whole cell lysate was incubated with magnetic anti-FLAG M2 beads (Sigma-Aldrich) for 1 h at 4°C, beads washed five times in immunoprecipitation buffer and protein eluted by heating to 80°C for 5 min in 3× SDS loading dye. Eluted proteins were then immunoblotted as per above.

RESULTS

NMR reveals distinct hSSB1 oligomerization interface

To determine the molecular details of oxidation-driven hSSB1 self-oligomerization (26,27), we initially recorded HSQC NMR experiments of hSSB1 under reducing (presence of 3 mM TCEP) and non-reducing conditions (absence of TCEP), respectively, and directly compared them to each other (Figure 1A). The protein construct that was used for these experiments encompassed the entire OB domain and a short part of the C-terminus (residues 1–123, $hSSB1_{1–123}$) and was previously shown to be sufficient for DNA binding (17). Apart from peak broadening indicative

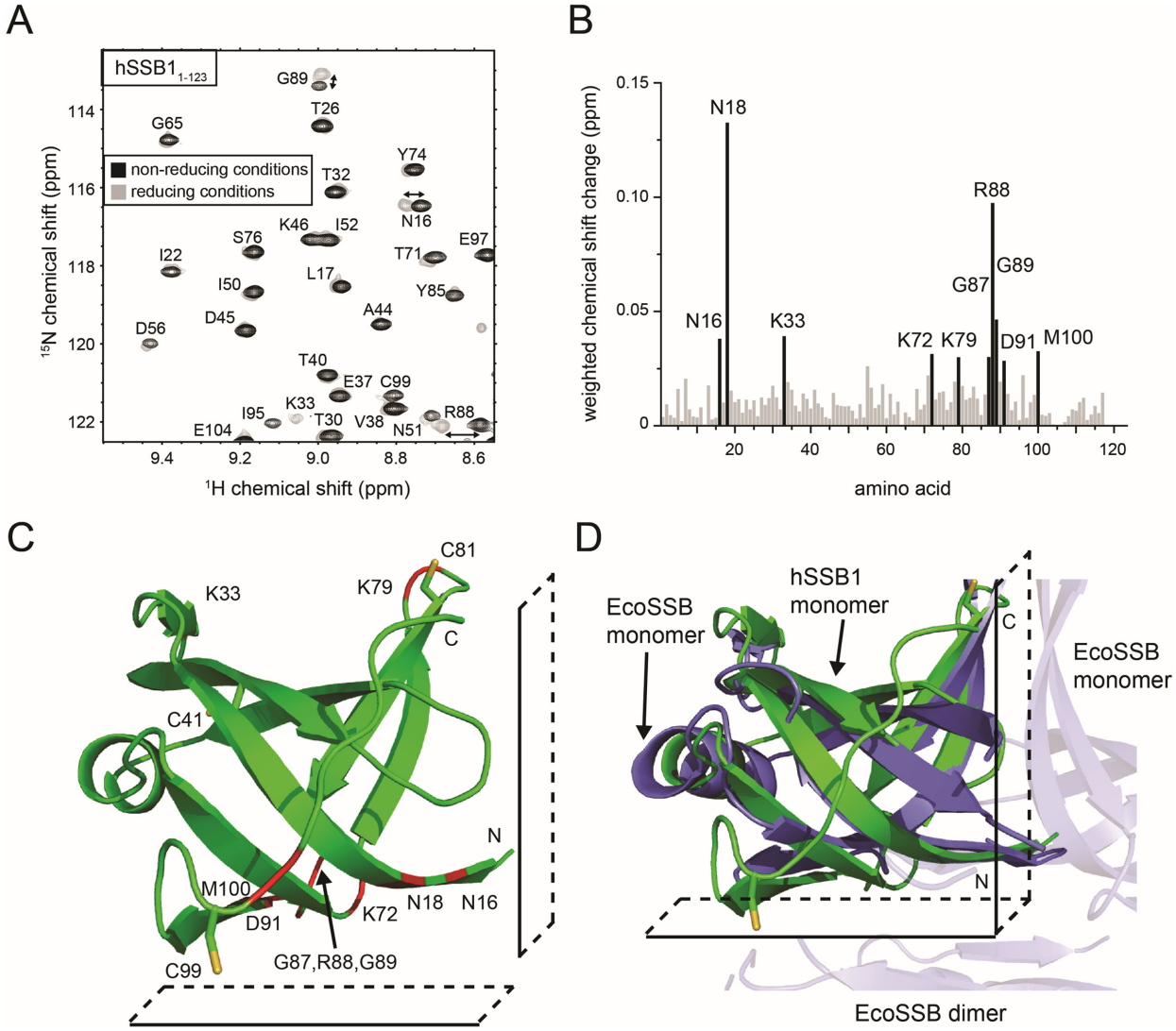

Figure 1. NMR analysis reveals the interaction surface of oxidation-driven hSSB1 oligomerisation. (**A**) Section of a ^{15}N-HSQC of $hSSB_{1–123}$ under reducing (light grey) and non-reducing conditions (black), respectively. Assignments and changes in backbone HN/N resonances are indicated. (**B**) Weighted backbone chemical shift changes (30) of HN and N atoms upon oligomer formation of hSSB1. Residues exhibiting changes larger than the average (surface residues) plus one standard deviation are coloured in black. (**C**) Cartoon representation of hSSB1 (taken from the published crystal structure, PDB ID: 4OWX) (19) with surface residues (as determined in B) coloured in red. Note that all surface residues apart from K33 are located on two distinct sides of hSSB1 (as indicated by rectangles). (**D**) Cartoon representation of an overlay of the tetrameric structure of *E. coli* SSB (EcoSSB, PDB ID: 1SRU) (34) onto hSSB1. Note the high structural similarity (RMSD of monomers = 1.66 Å) and the conservation of the interaction surface (rectangles) utilized in oligomer formation between hSSB1 and EcoSSB. hSSB1 is shown in the same orientation as in C.

of oligomer formation in the spectrum recorded under non-reducing conditions, we were also able to observed significant differences in the position of some NMR signals (Figure 1A).

Next, using the backbone assignments determined earlier (18) we calculated the differences in the chemical shifts of all backbone resonances between the spectra (Figure 1B). Notably, 10 residues exhibited substantial chemical shift differences (N16, N18, K33, K72, K79, G87, R88, G89, D91 and M100) which we mapped onto the existing crystal structure of hSSB1 (19) (Figure 1C). These data revealed that with the exception of K33 all residues are located on two distinct sides of the protein (as indicated in Figure 1C) that include both C81 and C99.

hSSB1 oligomerization is driven by cysteines C81 and C99

Our recently published study has revealed the presence of distinct hSSB1 monomers, dimers and tetramers under oxidizing conditions (26). We have also shown that cysteine 41 plays an important role in the self-oligomerization process of the protein, however, we have concluded that this residue is not able to form any oxidation-driven disulfide bonds, as its side chain is buried deeply within the hydrophobic core of the OB domain (19).

To further investigate the possibility that the remaining two cysteine residues (C81 and C99), which are surface-exposed, are involved in oligomer-formation we made three point mutations (C81S, C99S and C81S/C99S) and anal-

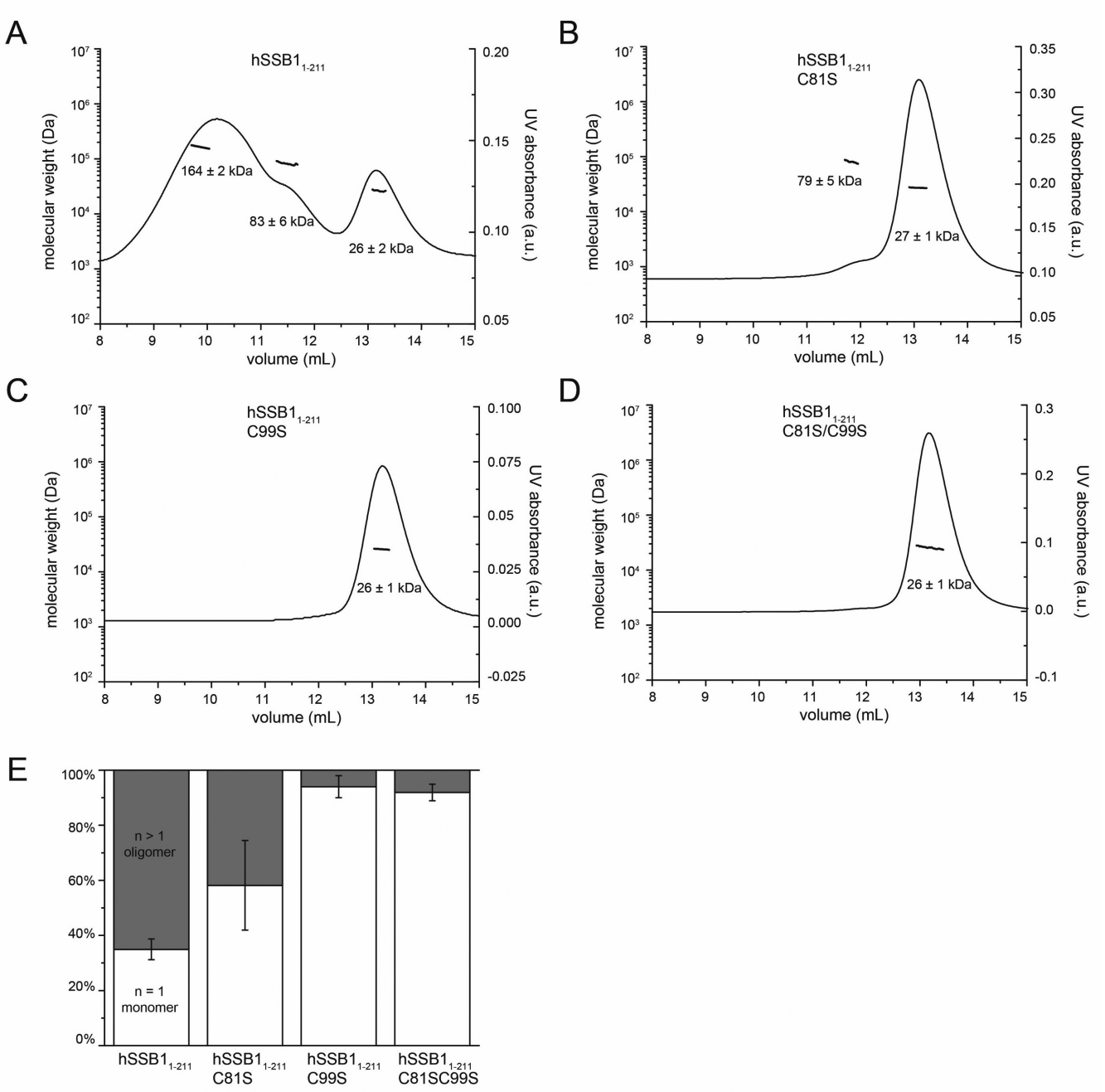

Figure 2. SEC-MALLS data confirm the involvement of cysteine residues C81 and C99 in the formation of hSSB1 oligomers. (**A–D**) Representative size-exclusion chromatography traces (lines) and MALLS data (dots) of full-length $hSSB_{1–211}$ and $hSSB1_{1–211}$ cysteine mutants in MALLS buffer under non-reducing conditions. (**E**) Summary of MALLS data ($n = 4–8$) displaying mass proportions of monomers versus oligomers for wild-type hSSB1 and cysteine mutants (250–500 μg).

ysed these mutant proteins under non-reducing conditions by size exclusion chromatography coupled with Multi-angle Laser Light Scattering (SEC-MALLS). All mutant proteins were assessed for correct folding by 1D NMR (Supplementary Figure S1). As seen previously (26), full-length hSSB1 ($hSSB1_{1–211}$) forms distinct monomers and higher oligomers, comprising of a mix of dimers, tetramers and larger oligomers (Figure 2A). In contrast, the C99S mutant occurs predominantly as a monomer in solution, whereas mutating C81 to a serine results in a significant reduction in the formation of higher oligomers (Figure 2B, C and E). Similarly, replacing both cysteines by serines (C81S/C99S) essentially abolished the ability of the protein to oligomerize (Figure 2D).

We could not detect significant chemical shifts of the backbone HN protons of either C81 or C99 in our NMR HSQC experiments (Figure 1), however, we were able to unambiguously assigned the signals of the side chain β-

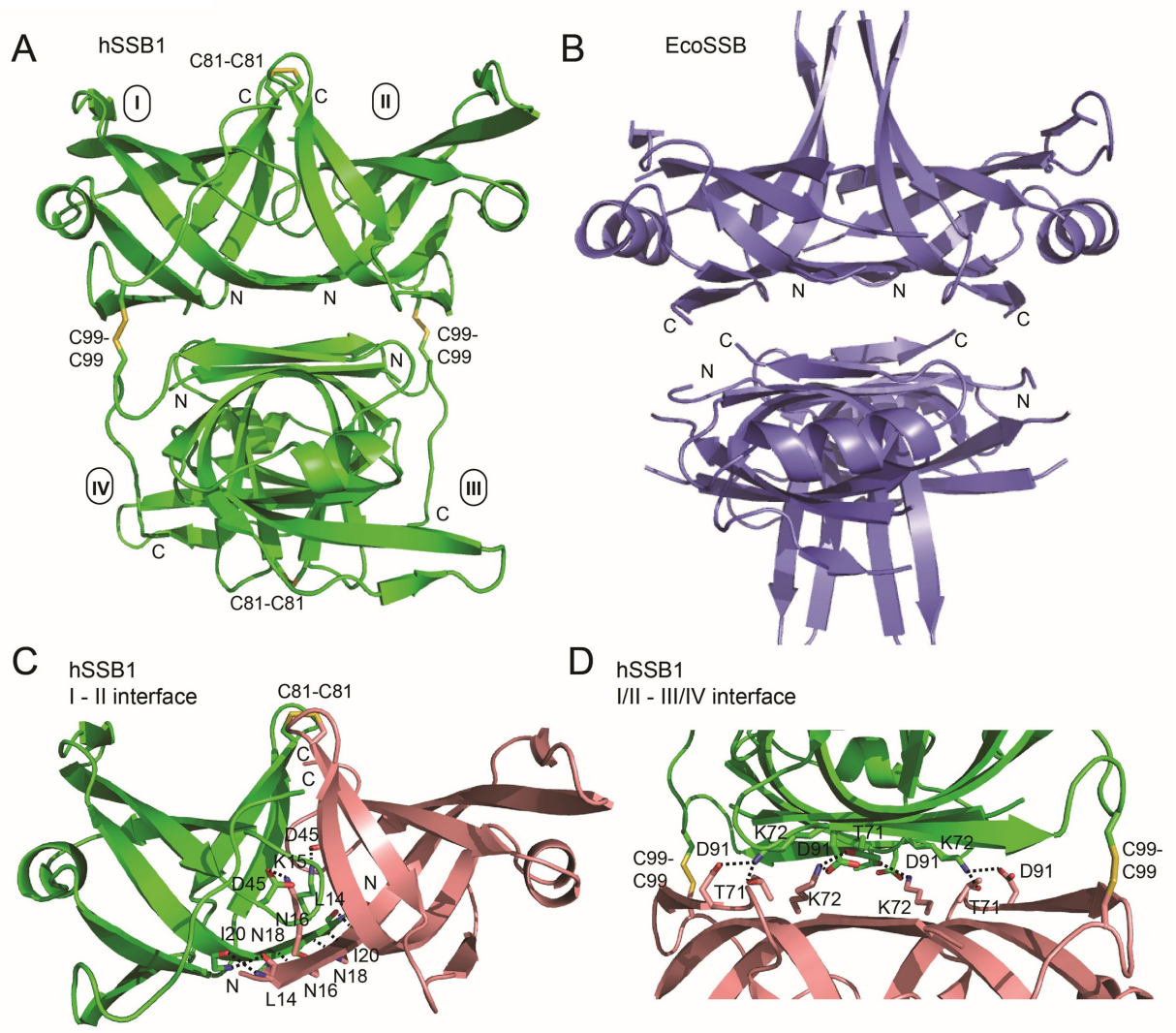

Figure 3. A data-driven structural model of hSSB1 oligomerization. (**A** and **B**) Cartoon representation of the energy-lowest hSSB1 HADDOCK structural model (coloured in green, shown in the same orientation as in Figure 1) and EcoSSB crystal structure (PDB ID 1SRU) (34) (dark-blue), respectively. The disulfide-forming cysteine residues C81 and C99 are indicated as sticks in hSSB1. Note the high structural similarity between the tetrameric hSSB1 and EcoSSB. (**C** and **D**) Details of the interface between molecules I and II (monomers coloured in green and salmon, respectively) as well as between molecules I/II and III/IV (dimers coloured in green and salmon, respectively) in the hSSB1 tetramer model. The side-chains of all surface residues that form electrostatic and hydrogen-bonds (black, dashed line) as well as C81 and C99 are indicated as sticks. In panel C, hSSB1 is shown in the same orientation as in Figure 1; in panel D, the structure has been rotated by 90° counter clockwise about the vertical axis when looking from above relative to Figure 1C.

protons of both residues using ^{13}C HSQC spectra and NMR data from our previously published study (17). Although assignment of these protons under non-reducing conditions was not possible, both signals disappear from their original position upon oxidation (Supplementary Figure S2), indicating a major change in the redox state of both C81 and C99 (36). Taken together, these data reveal that both C81 and C99 are important in oligomer formation, most likely via disulfide bonding between two or more hSSB1 molecules.

A data-driven model of hSSB1 oligomerization

To address the oligomerization capacity of hSSB1 visually, we next compared the interaction interface between individual hSSB1 molecules as determined by NMR (Figure 1C) with other structurally similar SSBs that form oligomers. Notably, a structural overlay of the hSSB1 OB domain monomer onto the *E. coli* (EcoSSB, PDB ID 1SRU) (34) OB domain tetramer (RMSD between monomers = 1.66 Å) reveals that EcoSSB utilizes the corresponding binding surface to form stable tetramers (Figure 1D). In the same manner, the intermolecular interaction interface is also conserved between hSSB1 and the dimeric (dimer of dimers) structure of the *Deinococcus radiodurans* SSB (DrSSB, PDB IDs 3UDG, RMSD between monomers = 1.76 Å) (37) (data not shown).

Based on these comparisons we utilized EcoSSB as a template in combination with our NMR and SEC-MALLS data to calculate a HADDOCK model of the hSSB1 tetramer (Figure 3A). To achieve this, we first calculated a

Table 1. Hydrophobic and electrostatic interactions (apart from cysteines C81 and C99) within the hSSB1 structural model

	Interface between molecules I and II	Interface between molecules I/II and III/IV
Hydrophobic	G13 ↔ M100 L14 ↔ L19 L17 ↔ L17 I50 ↔ V77 L82 ↔ L82	L14 ↔ T71 G89 ↔ G89 I20 ↔ I20
Electrostatic	K15 ↔ D45	T71 ↔ K72 K72 ↔ D91 K72 ↔ G89

dimer between two hSSB1 molecules (referred to as I and II) mediated by C81, residues located on the interface as identified by NMR experiments (Figure 1), and β-strands between residues L14, N16, N18 and I20 in analogy to EcoSSB (Figure 3C). In the second step, two dimers (referred to as I/II and III/IV) were docked together using C99 and interface residues (Figure 1) to form a stable tetramer *in silico*. Figure 3A depicts the lowest energy tetrameric structure calculated from a total of 500 HADDOCK structures. The interface between molecules I and II is, apart from the adjacent β-strands and the C81–C81 disulfide bond, stabilised by multiple hydrophobic contacts and one electrostatic interaction (Figure 3C, Table 1, Supplementary Figure S3), whereas the dimer interface (I/II–III/IV) is made up by both charged and hydrophobic residues and the C99–C99 disulfide bond (Figure 3D, Table 1, Supplementary Figure S3).

Evaluation of the hSSB1 tetramer model

Based on our ^{15}N-HSQC data and a visual examination of our structural model, we made a series of point mutations in $hSSB1_{1–211}$ to assess the validity of our data-driven HADDOCK model. The first two double-mutants were designed to disrupt formation of the β-strand (Figure 3C) that is integral to formation of the I/II dimer (N16D/N18D and L14DI20D), whereas in the third mutant we replaced two charged residues (K72 and D91) by alanines in an effort to disrupt the interface between molecules I/II and III/IV (Figure 3D). All three double-mutants were correctly folded as judged by their 1D NMR spectra (Supplementary Figure S1).

Next, the ability of each mutant to form oligomers under non-reducing conditions was assessed by SEC-MALLS, in analogy to Figure 2. As can be seen from Figure 4, all three double-mutations significantly reduced the formation of oligomers. Interestingly, replacing N16 and N18, which are located in the centre of the adjacent β-strands, by negatively charged aspartic acids, leads to a complete loss in the ability to form oligomers (Figure 4A and D), highlighting the role that this continuing β-sheet plays in the formation of hSSB1 oligomers. In summary, these data confirm the validity of our structural model.

Functional data further validate the structural model

To further corroborate our structural model we examined whether mutation of residues important for tetramer formation impacted oligomerisation of hSSB1 in cells. Three $hSSB1_{1–211}$ mutants (N16D/N18D/K72A/D91A, C81S/C99S and N16D/N18D/K72A/D91A/C81S/C99S) were made and ectopically expressed in HeLa cells grown at 2% oxygen and treated with or without H_2O_2. Whole cell lysates were then collected and analysed by immunoblotting under non-reducing and reducing conditions (Figure 5A). While mutation of N16 and N18 (part of β-sheet), together with K72 and D91 (part of the dimer-dimer interface) did result in significantly reduced ratios between oligomer and monomer compared to the wild-type (Figure 5A, left), additionally replacing the two surface-exposed cysteines C81 and C99 with serines completely abolished the formation of hSSB1 oligomers (Figure 5A, far right) in good agreement with our HADDOCK model. Consistent with our MALLS data (Figure 2E), mutation of the two cysteines almost eliminates any oligomeric species, with only small amounts of dimer compared to the monomer still visible on the gel (Figure 5A, middle).

We additionally carried out clonogenic survival assays using HeLa cells treated with increasing concentrations of H_2O_2 (to induce oxidative DNA damage) depleted of endogenous full-length $hSSB1_{1–211}$ and transiently expressing siRNA resistant full-length 3× FLAG tagged wild-type $hSSB1_{1–211}$, or C81S/C99S, N16D/N18D/K72A/D91A, and N16D/N18D/K72A/D91A/C81S/C99S mutants (Figure 5B). We have previously found that oligomerisation of hSSB1 is required for cell survival following H_2O_2 treatment (26,27). In agreement with this, expression of wild-type hSSB1 was able to rescue depletion of endogenous hSSB1. However, mutation of either the two cysteines C81 and C99 or a combination of the cysteines with N16, N18, K72 and D91 led to a significant decreased cell survival compared to the control. Taken together, these functional data provide further strong evidence for the validity of our structural model.

hSSB1 binding to SOSS1 complex does not interfere with oligomerization

hSSB1 has previously been shown to form a hetero-trimeric complex with Ints3 and C9orf80 (SOSS1 complex), facilitating the function of hSSB1 in DSB repair and in controlling the termination of transcription (20,22,23,38). It is not clear whether Ints3 binding within the SOSS1 complex would interfere with hSSB1 self-oligomerization (and thus oxidative DNA damage repair). To assess this, we initially overlaid the existing Int3–hSSB1–ssDNA complex structure (PDB ID 4OWX) (19) onto our tetramer model (Figure 6A, shown without hSSB1 and ssDNA from the complex structure). Intriguingly, no clash between Ints3 and hSSB1 is observed in the structure, indicating that Ints3 binding

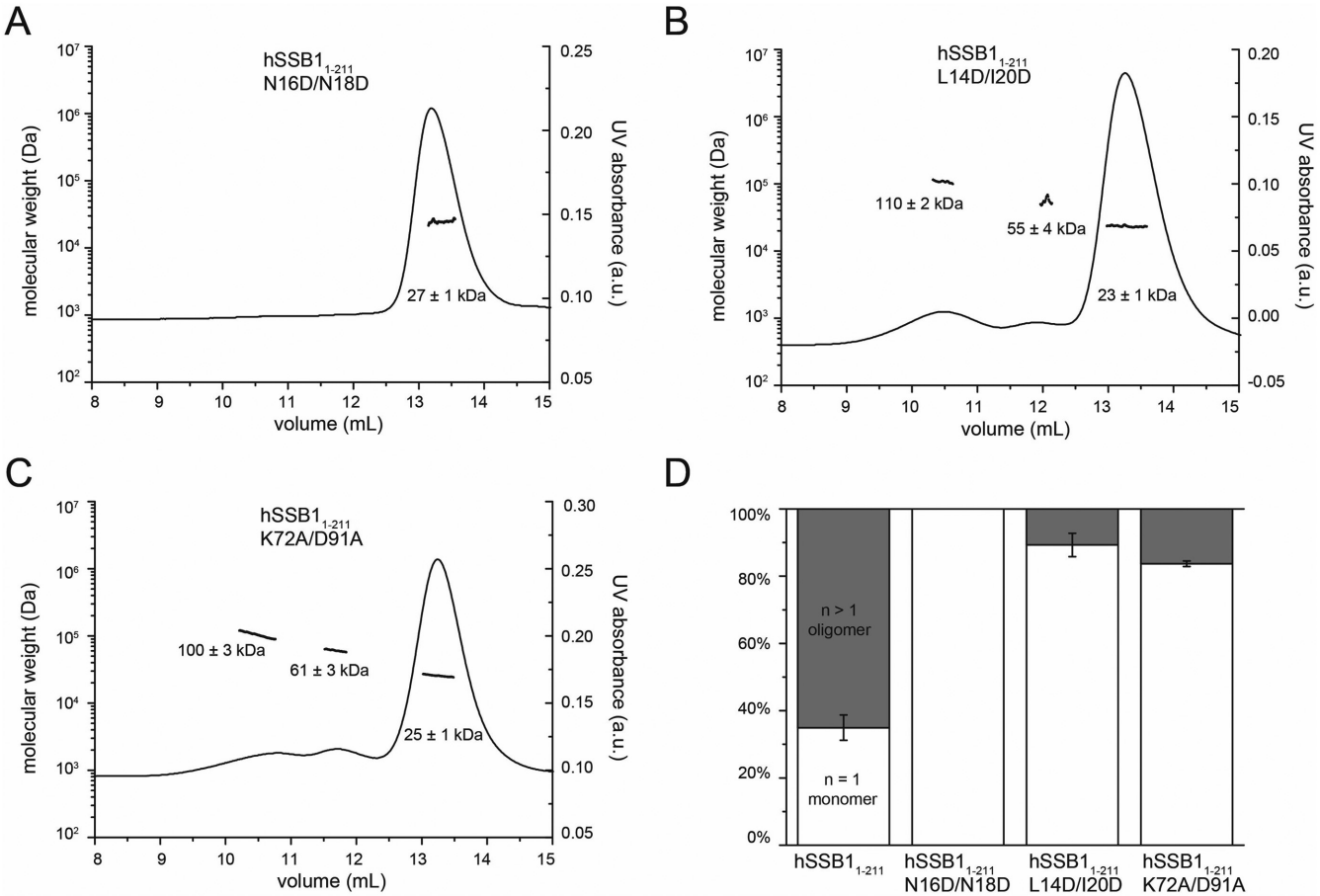

Figure 4. SEC-MALLS experiments confirm the validity of the structural model. (**A–C**) Representative size-exclusion chromatography traces and MALLS data of $hSSB1_{1–211}$ surface residue mutants in MALLS buffer. (**D**) Summary of MALLS data ($n = 3–4$) displaying mass proportions of monomers versus oligomers for wild-type hSSB1 and mutant proteins.

may be able to take place independently of hSSB1 oligomerization.

To confirm this in cells, we assessed the ability of two $hSSB1_{1–211}$ mutants (C81S/C99S and N16D/N18D/K72A/K91A) that affect hSSB1 oligomerization to bind Ints3 in immunoprecipitation experiments (Figure 6B, left four lanes). Albeit reduced in the case of the double cysteine mutant, both hSSB1 constructs are still able to interact with Ints3. In contrast, replacing F98 in hSSB1, a residue that makes extensive contacts with Ints3 in the crystal structure (19), with alanine, completely abolishes hSSB1 binding to Ints3.

To further confirm that Ints3 binding can take place independently of hSSB1 oligomerization, we first tested whether the F98A mutant is able to rescue cells depleted of endogenous full-length hSSB1 that were exposed to oxidative DNA damage (Figure 5B). As seen from the Figure, the cell surviving fraction is identical to the wild-type protein indicating that this mutant, while unable to bind Ints3, is still fully functional in BER repair. Secondly, we tested for the presence of oligomers in immunoblots revealing that this mutant displays oligomerization capacity identical to the wild-type protein (no significant difference in the ratios between oligomer and monomer, Figure 6C). In summary, our data indicate that two distinct hSSB1 interfaces (that do not overlap) are utilized for Ints3 binding and self-oligomerization, respectively.

DISCUSSION

The role of the cysteine residues in hSSB1 oligomer formation

Our data-driven hSSB1 tetramer model provides crucial insight into how hSSB1 oligomerizes which is an important prerequisite for its function in the oxidative damage pathway (26,27). Protein self-oligomerization is often associated with the formation of intermolecular disulfide bonds between cysteines. While we have recently shown that C41 plays an important role in hSSB1 oligomer formation (26), in light of our structural model it is now clear that, while not directly involved in disulfide formation, this cysteine must act as a redox-sensing cysteine with its oxidative status influencing the structure of the protein. The other two cysteines, C81 and C99, however, are surface exposed and most likely form intermolecular S-S bridges that stabilize the tetramer as observed in our tetramer model. While the formation of these disulfide bonds is strongly supported by our MALLS and NMR data, we were unable to detect them by X-ray crystallography as attempts to grow viable crys-

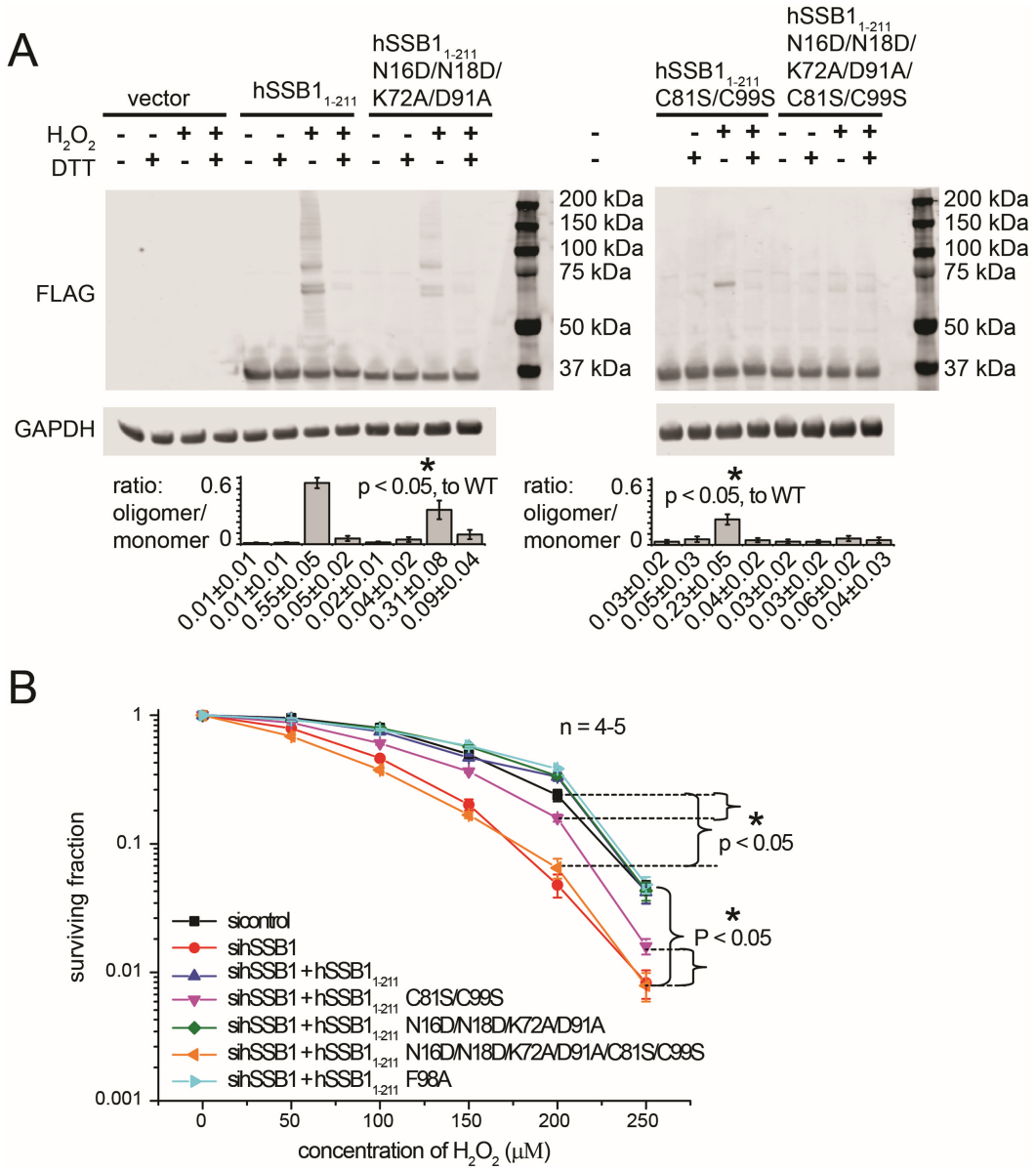

Figure 5. Functional experiments in cells further corroborate structural data. (**A**) Immunoblots of lysates from HeLa cells transfected with vector alone, 3× FLAG wild type $hSSB1_{1–211}$ or 3× FLAG $hSSB1_{1–211}$ mutants and left untreated or treated with 250 μM H_2O_2 in the presence or absence of DTT. Calculated ratios between oligomer and monomer (signal intensities of corresponding protein bands) for each lane taken from three different blots (average ± standard error) are shown. Note that oligomer formation is abolished for the N16D/N18D/K72A/D91A/C81S/C99S mutant and significantly reduced for the other two mutants. (**B**) Survival curves from a clonogenic assay of HeLa cells depleted for hSSB1 (full-length) and challenged by oxidative stress (H_2O_2 treatment). Non-depleting negative control (scramble, black), sihSSB1 (red), siRNA-resistant flag-tagged hSSB1 (+hSSB1, blue) and siRNA-resistant flag-tagged hSSB1 mutants (+$hSSB1_{1–211}$ C81S/C99S, purple; +$hSSB1_{1–211}$ N16D/N18D/K72A/D91A, green; +$hSSB1_{1–211}$ N16D/N18D/K72A/D91A/C81S/C99S, orange and +$hSSB1_{1–211}$ F98A, light-blue), respectively, were transfected into cells. All points represent the mean ± standard error from four to five independent experiments. Note the significant difference between cell surviving fraction of control and the C81SC99S as well as the N16D/N18D/K72A/D91A/C81S/C99S mutant both at 200 and 250 μM H_2O_2 ($P < 0.05$).

tals were unsuccessful, most likely due to the presence of a mix of different subspecies (monomers, dimers, and higher oligomers) as seen in our MALLS data of wild-type hSSB1 proteins (Figure 2A). Interestingly, while SSBs are generally well known to form homotetramers (39), disulfide bonds have recently been shown to be essential in the formation of stable tetramers by the SSB from *Streptomyces coelicolor* (40). Similar to hSSB1, the presence of reducing agent completely abolishes tetramer formation of this SSB. These data indicate that intermolecular S–S bridges that stabilize tetrameric structures might be a necessary requirement for the biological function of SSBs important in oxidative stress response pathways.

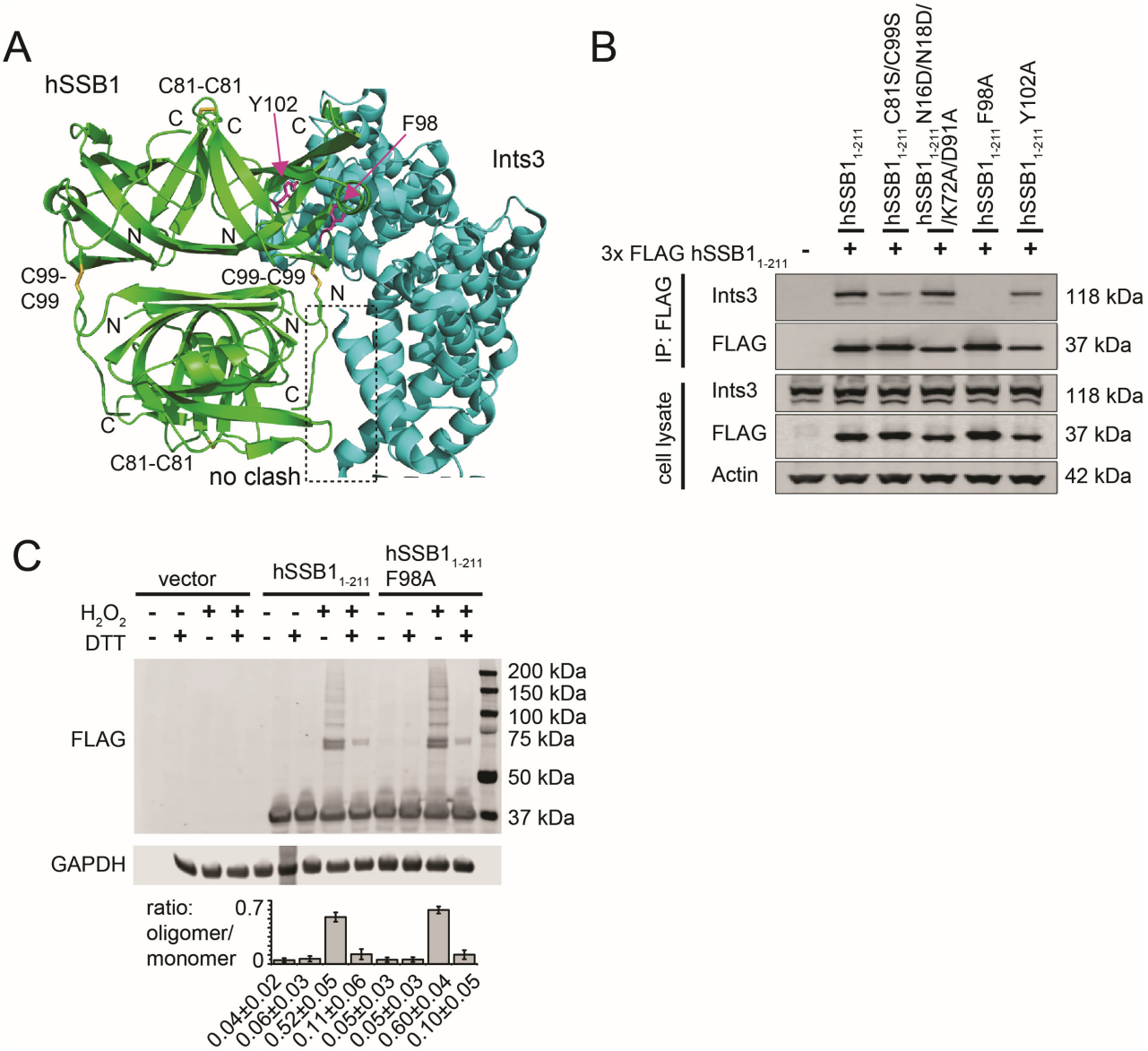

Figure 6. hSSB1 utilizes two distinct non-overlapping interfaces for SOSS1 binding and oligomerization, respectively. (**A**) Cartoon representation of an overlay of the hSSB1–Ints–ssDNA complex structure (PDB ID: 4OWX, Ints3 coloured in light-blue, hSSB1 and ssDNA from complex structure are omitted for clarity) (19) onto the hSSB1 tetramer model (same orientation as in Figure 3). Note that no clashes are observed in the overlay (as indicated). (**B**) Immunoprecipitation of FLAG-tagged proteins from untreated HeLa cells co-expressing 3× FLAG-hSSB1$_{1–211}$ or 3× FLAG-hSSB1$_{1–211}$ mutants with Ints3. Samples were analysed by immunoblotting with the indicated antibodies. Note that both mutants that affect oligomer formation (C81S/C99S and N16D/N18D/K72A/D91D) are still able to bind Ints3. (**C**) Immunoblots of lysates from HeLa cells transfected with vector alone, 3× FLAG wild type hSSB1$_{1–211}$ or 3× FLAG hSSB1$_{1–211}$ F98A mutant and left untreated or treated with 250 μM H_2O_2 in the presence or absence of DTT. Calculated ratios between oligomer and monomer (signal intensities of corresponding protein bands) for each lane taken from three different blots (average ± standard error) are shown. Note that the hSSB1$_{1–211}$ F98A mutant (deficient in Ints3 binding, see above) forms oligomers analogous to the wild-type protein.

The data-driven model tetramer model is structurally similar to other tetrameric SSBs

Apart from the two cysteine residues that appear to act as molecular clamps, we have identified both hydrophilic and hydrophobic residues that are essential in the formation of hSSB1 tetramers (Table 1). Comparison of surface residues of hSSB1 with both the SSB from *Deinococcus radiodurans* (DrSSB, Supplementary Figure S3A and B) and *E. coli* (EcoSSB, Supplementary Figure S3C), respectively, reveals two important common features. Firstly, the majority of intermolecular interactions are made involving a stretch of ∼10 residues at the N-terminus of the OB domain. These residues take part in the continuous β-sheet formation between molecules I and II as well as several electrostatic and hydrophobic contacts that stabilize the tetramer (for hSSB1 see Table 1). Secondly, while the nature of the interactions varies between hSSB1 and the other two SSBs, the location of the participating residues appears to be mostly conserved. For example, whereas hSSB1 utilizes C81 and L82 to make disulfide bonds and hydrophobic contacts between

molecules I and II (see Figure 3), the structurally equivalent interactions in EcoSSB are formed between the negatively charged D96 and the positively charged R97. Moreover, several known residues that affect tetramer formation when mutated in EcoSSB (12) are at similar positions to ones in hSSB1 that we have shown to be important for oligomerization (H56, Q77, Q111; underlined in Supplementary Figure S3C). Despite these structural similarities it has to be noted that hSSB1, in contrast to other SSBs, exists in solution in multiple oligomeric states which is an essential prerequisite for its function in the different DNA repair pathways (22–27). Importantly, both our MALLS and functional data (Figures 2A and 5A) indicate that hSSB1 tetramers might be capable of polymerizing into larger oligomers of unknown function by binding additional protein monomers.

Oligomer formation of hSSB1 does not preclude involvement in DSB repair response

hSSB1 is part of two well-characterized multi-protein complexes that are essential for DNA DSB repair (SOSS1 and MRN complex) (20–25). Whereas Ints3 in the SOSS1 complex contacts the OB domain of hSSB1 directly, protein binding in the MRN complex is via the flexible carboxyl tail of hSSB1. Our structural model of hSSB1 oligomerization (Figure 3) has revealed that only the OB domain is required for the formation of tetramers with no contribution of the flexible carboxyl-tail implying that oligomer formation does not interfere with MRN binding. Similarly, our IP, immunoblot and cell survival experiments (Figures 5 and 6) indicate that binding of hSSB1 to itself does not interfere with recognition of Ints3 (as part of the SOSS1 complex), in good agreement with our previous results (26). Taken together, these data show that hSSB1 may be able to function in BER and in the HR-modulated DSB repair pathway simultaneously, further establishing the importance and versatility that hSSB1 displays in maintaining genome integrity.

DNA binding of hSSB1

We have recently revealed how monomeric hSSB1 is able to recognise ssDNA and demonstrated that the binding mode in solution is different from the one found in the SOSS1 crystal structure (17,19). The defining feature of the hSSB1–ssDNA complex solution structure is the base-stacking of four aromatic residues (W55, Y74, F78, F85), none of which are directly involved in self-oligomerization, indicating that ssDNA binding by hSBB1 does not interfere with tetramer formation. These data raise the possibility that oligomeric hSSB1 might interact with ssDNA or dsDNA as a functional tetramer, similar to EcoSSB (12,41). Further structural and biophysical studies are required in order to establish the exact binding mode of oligomeric hSSB1; in particular whether it is able to adopt different binding modes analogous to EcoSSB (41). The increased binding affinity that hSSB1 displays when recognizing dsDNA containing a single 8-oxoG (26) might be due to a change in hSSB1 binding modality. Different DNA binding modalities have been reported for several SSBs. For example, both RPA and EcoSSB have been shown to exhibit multiple ssDNA binding modes, accompanied by conformational changes that are central to their function in ssDNA processing mechanisms (1,42,43).

In conclusion, our structural model describes how hSSB1 is able to oligomerize by forming stable tetramers, a process that is dependent on oxidation and driven by the two surface-exposed cysteine residues C81 and C99. Our structural analysis also reveals that the interaction of hSSB1 with Ints3 (as part of SOSS1 complex) does not interfere with tetramer formation, indicating that these two processes can occur independently from each other in the cell. Future biophysical and functional experiments will aim at confirming this, as well as determining the structural basis of DNA recognition by hSSB1 tetramers. The data presented here is central to understanding the molecular mechanism of oxidation-dependent oligomer formation of hSSB1 in the context of oxidative DNA damage repair, particularly since blocking this process in tumour cells may be of significant interest for the development of novel cancer therapeutics.

SUPPLEMENTARY DATA

Supplementary Data are available at NAR Online.

ACKNOWLEDGEMENTS

We would like to thank Dr Ann Kwan from the University of Sydney for expert advice and maintenance of NMR spectrometers.

FUNDING

NHMRC [1066540 to L.C.]; NHMRC Early Career Fellowship [1091589 to M.N.A.]. Funding for open access charge: Western Sydney University.
Conflict of interest statement. None declared.

REFERENCES

1. Shereda,R.D., Kozlov,A.G., Lohman,T.M., Cox,M.M. and Keck,J.L. (2008) SSB as an organizer/mobilizer of genome maintenance complexes. *Crit. Rev. Biochem. Mol. Biol.*, **43**, 289–318.
2. Cubeddu,L., Richard,D.J., Bolderson,E., White,M.F. and Khanna,K.K. (2008) hSSB1, an evolutionary conserved single stranded DNA binding protein critical for the DNA damage response. *FEBS J.*, **275**, 201–201.
3. Richard,D.J., Bolderson,E., Cubeddu,L., Wadsworth,R.I.M., Savage,K., Sharma,G.G., Nicolette,M.L., Tsvetanov,S., McIlwraith,M.J., Pandita,R.K. *et al.* (2008) Single-stranded DNA-binding protein hSSB1 is critical for genomic stability. *Nature*, **453**, 677–681.
4. Ashton,N.W., Bolderson,E., Cubeddu,L., O'Byrne,K.J. and Richard,D.J. (2013) Human single-stranded DNA binding proteins are essential for maintaining genomic stability. *BMC Mol. Biol.*, **14**, 9.
5. Richard,D.J., Bolderson,E. and Khanna,K.K. (2009) Multiple human single-stranded DNA binding proteins function in genome maintenance: structural, biochemical and functional analysis. *Crit. Rev. Biochem. Mol. Biol.*, **44**, 98–116.
6. Iftode,C., Daniely,Y. and Borowiec,J.A. (1999) Replication protein A (RPA): The eukaryotic SSB. *Crit. Rev. Biochem. Mol. Biol.*, **34**, 141–180.
7. Wold,M.S. (1997) Replication protein A: a heterotrimeric, single-stranded DNA-binding protein required for eukaryotic DNA metabolism. *Annu. Rev. Biochem.*, **66**, 61–92.
8. Bochkareva,E., Korolev,S., Lees-Miller,S.P. and Bochkarev,A. (2002) Structure of the RPA trimerization core and its role in the multistep DNA-binding mechanism of RPA. *EMBO J.*, **21**, 1855–1863.

9. Brill,S.J. and Bastin-Shanower,S. (1998) Identification and characterization of the fourth single-stranded-DNA binding domain of replication protein A. *Mol. Cell. Biol.*, **18**, 7225–7234.
10. Morten,M.J., Peregrina,J.R., Figueira-Gonzalez,M., Ackermann,K., Bode,B.E., White,M.F. and Penedo,J.C. (2015) Binding dynamics of a monomeric SSB protein to DNA: a single-molecule multi-process approach. *Nucleic Acids Res.*, **43**, 10907–10924.
11. Lohman,T.M. and Ferrari,M.E. (1994) Escherichia coli single-stranded DNA-binding protein—multiple DNA-binding modes and cooperativities. *Annu. Rev. Biochem.*, **63**, 527–570.
12. Raghunathan,S., Ricard,C.S., Lohman,T.M. and Waksman,G. (1997) Crystal structure of the homo-tetrameric DNA binding domain of Escherichia coli single-stranded DNA-binding protein determined by multiwavelength x-ray diffraction on the selenomethionyl protein at 2.9-angstrom resolution. *Proc. Natl. Acad. Sci. U.S.A.*, **94**, 6652–6657.
13. Gamsjaeger,R., Kariawasam,R., Gimenez,A.X., Touma,C., McIlwain,E., Bernardo,R.E., Shepherd,N.E., Ataide,S.F., Dong,Q., Richard,D.J. *et al.* (2015) The structural basis of DNA binding by the single-stranded DNA-binding protein from Sulfolobus solfataricus. *Biochem. J.*, **465**, 337–346.
14. Kerr,I.D., Wadsworth,R.I.M., Cubeddu,L., Blankenfeldt,W., Naismith,J.H. and White,M.F. (2003) Insights into ssDNA recognition by the OB fold from a structural and thermodynamic study of Sulfolobus SSB protein. *EMBO J.*, **22**, 2561–2570.
15. Cubeddu,L. and White,M.F. (2005) DNA damage detection by an archaeal single-stranded DNA-binding protein. *J. Mol. Biol.*, **353**, 507–516.
16. Wadsworth,R.I. and White,M.F. (2001) Identification and properties of the crenarchaeal single-stranded DNA binding protein from Sulfolobus solfataricus. *Nucleic Acids Res.*, **29**, 914–920.
17. Touma,C., Kariawasam,R., Gimenez,A.X., Bernardo,R.E., Ashton,N.W., Adams,M.N., Paquet,N., Croll,T.I., O'Byrne,K.J., Richard,D.J. *et al.* (2016) A structural analysis of DNA binding by hSSB1 (NABP2/OBFC2B) in solution. *Nucleic Acids Res.*, **44**, 7963–7973.
18. Kariawasam,R., Touma,C., Cubeddu,L. and Gamsjaeger,R. (2016) Backbone (1)H, (13)C and (15)N resonance assignments of the OB domain of the single stranded DNA-binding protein hSSB1 (NABP2/OBFC2B) and chemical shift mapping of the DNA-binding interface. *Biomol. NMR Assign.*, **10**, 297–300.
19. Ren,W.D., Chen,H.X., Sun,Q.Z., Tang,X.H., Lim,S.C., Huang,J. and Song,H.W. (2014) Structural basis of SOSS1 complex assembly and recognition of ssDNA. *Cell Rep.*, **6**, 982–991.
20. Huang,J., Gong,Z., Ghosal,G. and Chen,J. (2009) SOSS complexes participate in the maintenance of genomic stability. *Mol. Cell*, **35**, 384–393.
21. Li,Y.J., Bolderson,E., Kumar,R., Muniandy,P.A., Xue,Y.T., Richard,D.J., Seidman,M., Pandita,T.K., Khanna,K.K. and Wang,W.D. (2009) hSSB1 and hSSB2 form similar multiprotein complexes that participate in DNA damage response. *J. Biol. Chem.*, **284**, 23525–23531.
22. Skaar,J.R., Ferris,A.L., Wu,X., Saraf,A., Khanna,K.K., Florens,L., Washburn,M.P., Hughes,S.H. and Pagano,M. (2015) The Integrator complex controls the termination of transcription at diverse classes of gene targets. *Cell Res.*, **25**, 288–305.
23. Skaar,J.R., Richard,D.J., Saraf,A., Toschi,A., Bolderson,E., Florens,L., Washburn,M.P., Khanna,K.K. and Pagano,M. (2009) INTS3 controls the hSSB1-mediated DNA damage response. *J. Cell Biol.*, **187**, 25–32.
24. Richard,D.J., Cubeddu,L., Urquhart,A., Bain,A., Bolderson,E., Menon,D., White,M.F. and Khanna,K.K. (2011) hSSB1 interacts directly with the MRN complex stimulating its recruitment to DNA double-strand beaks and its endo-nuclease activity. *Nucleic Acids Res.*, **39**, 3643–3651.
25. Richard,D.J., Savage,K., Bolderson,E., Cubeddu,L., So,S., Ghita,M., Chen,D.J., White,M.F., Richard,K., Prise,K.M. *et al.* (2010) hSSB1 rapidly binds at the site of DNA double-strand breaks and is required for the effecient recruitment of the MRN complex. *Nucleic Acids Res.*, **39**, 1692–1702.
26. Paquet,N., Adams,M.N., Ashton,N.W., Touma,C., Gamsjaeger,R., Cubeddu,L., Leong,V., Beard,S., Bolderson,E., Botting,C.H. *et al.* (2016) hSSB1 (NABP2/OBFC2B) is regulated by oxidative stress. *Scientific Rep.*, **6**, 27446.
27. Paquet,N., Adams,M.N., Leong,V., Ashton,N.W., Touma,C., Gamsjaeger,R., Cubeddu,L., Beard,S., Burgess,J.T., Bolderson,E. *et al.* (2015) hSSB1 (NABP2/ OBFC2B) is required for the repair of 8-oxo-guanine by the hOGG1-mediated base excision repair pathway. *Nucleic Acids Res.*, **43**, 8817–8829.
28. Cai,M., Huang,Y., Sakaguchi,K., Clore,G.M., Gronenborn,A.M. and Craigie,R. (1998) An efficient and cost-effective isotope labeling protocol for proteins expressed in Escherichia coli. *J. Biomol. NMR*, **11**, 97–102.
29. Cubeddu,L., Joseph,S., Richard,D.J. and Matthews,J.M. (2012) Contribution of DEAF1 structural domains to the interaction with the breast cancer oncogene LMO4. *PLoS One*, **7**, e39218.
30. Ayed,A., Mulder,F.A., Yi,G.S., Lu,Y., Kay,L.E. and Arrowsmith,C.H. (2001) Latent and active p53 are identical in conformation. *Nat. Struct. Biol.*, **8**, 756–760.
31. Ren,W., Chen,H., Sun,Q., Tang,X., Lim,S.C., Huang,J. and Song,H. (2014) Structural basis of SOSS1 complex assembly and recognition of ssDNA. *Cell Rep.*, **6**, 982–991.
32. de Vries,S.J., van Dijk,A.D., Krzeminski,M., van Dijk,M., Thureau,A., Hsu,V., Wassenaar,T. and Bonvin,A.M. (2007) HADDOCK versus HADDOCK: new features and performance of HADDOCK2.0 on the CAPRI targets. *Proteins*, **69**, 726–733.
33. Dominguez,C., Boelens,R. and Bonvin,A.M. (2003) HADDOCK: a protein-protein docking approach based on biochemical or biophysical information. *J. Am. Chem. Soc.*, **125**, 1731–1737.
34. Savvides,S.N., Raghunathan,S., Futterer,K., Kozlov,A.G., Lohman,T.M. and Waksman,G. (2004) The C-terminal domain of full-length E. coli SSB is disordered even when bound to DNA. *Protein Sci.*, **13**, 1942–1947.
35. Berman,H.M., Burley,S.K., Chiu,W., Sali,A., Adzhubei,A., Bourne,P.E., Bryant,S.H., Dunbrack,R.L. Jr, Fidelis,K., Frank,J. *et al.* (2006) Outcome of a workshop on archiving structural models of biological macromolecules. *Structure*, **14**, 1211–1217.
36. Sharma,D. and Rajarathnam,K. (2000) 13C NMR chemical shifts can predict disulfide bond formation. *J. Biomol. NMR*, **18**, 165–171.
37. George,N.P., Ngo,K.V., Chitteni-Pattu,S., Norais,C.A., Battista,J.R., Cox,M.M. and Keck,J.L. (2012) Structure and cellular dynamics of Deinococcus radiodurans single-stranded DNA (ssDNA)-binding protein (SSB)-DNA complexes. *J. Biol. Chem.*, **287**, 22123–22132.
38. Zhang,F., Ma,T. and Yu,X. (2013) A core hSSB1-INTS complex participates in the DNA damage response. *J. Cell Sci.*, **126**, 4850–4855.
39. Dickey,T.H., Altschuler,S.E. and Wuttke,D.S. (2013) Single-stranded DNA-binding proteins: multiple domains for multiple functions. *Structure*, **21**, 1074–1084.
40. Paradzik,T., Ivic,N., Filic,Z., Manjasetty,B.A., Herron,P., Luic,M. and Vujaklija,D. (2013) Structure-function relationships of two paralogous single-stranded DNA-binding proteins from Streptomyces coelicolor: implication of SsbB in chromosome segregation during sporulation. *Nucleic Acids Res.*, **41**, 3659–3672.
41. Raghunathan,S., Kozlov,A.G., Lohman,T.M. and Waksman,G. (2000) Structure of the DNA binding domain of E. coli SSB bound to ssDNA. *Nat. Struct. Biol.*, **7**, 648–652.
42. Brosey,C.A., Yan,C., Tsutakawa,S.E., Heller,W.T., Rambo,R.P., Tainer,J.A., Ivanov,I. and Chazin,W.J. (2013) A new structural framework for integrating replication protein A into DNA processing machinery. *Nucleic Acids Res.*, **41**, 2313–2327.
43. Fanning,E., Klimovich,V. and Nager,A.R. (2006) A dynamic model for replication protein A (RPA) function in DNA processing pathways. *Nucleic Acids Res.*, **34**, 4126–4137.